

Difference in Enhancement Between Spin Echo and 3-Dimensional Fast Spoiled Gradient Recalled Acquisition in Steady State Magnetic Resonance Imaging of Brain Metastasis at 3-T Magnetic Resonance Imaging

Kaori Furutani, MD,* Masafumi Harada, MD, PhD,† Mahmut Mawlan, MD,*
and Hiromu Nishitani MD, PhD*

Objective: To compare the enhancement of brain metastasis between 3-dimensional fast spoiled gradient recalled acquisition in the steady state (3DFSPGR) and spin echo (SE) T1-weighted imaging at 3-T magnetic resonance imaging.

Methods: The subjects comprised 18 patients with 81 suspected brain metastases. Axial SE and 3DFSPGR images were obtained before and after gadoteridol injection. The signal intensity of each tumor was measured for each sequence; the enhancement and contrast rates were also calculated.

Results: For equivalent slice thicknesses, the enhancement and contrast rates of the 3DFSPGR images were lower than those of the SE images (<0.05), whereas for the thin slices, the rates were higher for the 3DFSPGR images ($P < 0.01$).

Conclusions: On 3-T magnetic resonance imaging, the enhancement of 3DFSPGR images was less than that of the SE images under the same conditions, but not to a fatal degree, and thin slice 3DFSPGR imaging is therefore considered to be useful for detecting small lesions, when given a high dose of contrast agent and a suitable scanning delay time.

Key Words: MRI, spin echo, FSPGR

(*J Comput Assist Tomogr* 2008;32:313–319)

High-field systems of more than 3-T magnetic resonance imaging (3T MRI) have been available for clinical use for several years. The advantage of the higher signal-to-noise ratio of 3T MRI contributes to an improvement in the spatial resolution. However, the T1 relaxation times of the gray and white matter tend to become longer, and the inhomogeneity of the radiofrequency field is increased at 3 T. These effects reduce the T1 contrast of the brain on conventional T1-weighted spin echo (SE) sequences without contrast agent administration as a disadvantage on 3 T in comparison with 1.5 T.¹ Instead of conventional T1-weighted SE sequences,

the opportunity to use the 3-dimensional fast spoiled gradient recalled acquisition in the steady state (3DFSPGR) sequence may be increased in clinical routine examinations at 3 T to acquire a high contrast T1-weighted image (T1-WI) between gray and white matters. Even in the case of contrast-enhanced T1-weighted examinations after contrast agent administration, 3DFSPGR is sometimes preferred because of the high resolution and the decrease in the partial volume phenomenon to detect small lesions.²

According to our previous experience at 3 T, however, we have found a number of cases in which the enhancement effect on fast spoiled gradient recalled acquisition in the steady state (FSPGR) was lower than that observed on the SE image, as shown in Figure 1. In past studies, some reports have shown a lower enhancement effect on gradient-echo (GE) sequences, such as spoiled gradient recalled acquisition in the steady state (SPGR), after gadolinium (Gd) contrast infusion than on conventional T1-weighted SE sequences by the clinical evaluation and theoretical simulation.^{3–7} Elster⁸ emphasized that all T1-weighted sequences are not equal in demonstrating contrast enhancement, and especially, SPGR sequences do not show the same degree of visually apparent contrast enhancement compared with conventional SE sequences. However, others have demonstrated almost the same or a higher detectability on the 3D-GE sequences in comparison with the conventional SE sequences.^{9–12}

Given our previous experience and the results of the past studies, we set up 2 hypotheses: (1) that the enhanced effect on 3DFSPGR sequence after contrast agent administration at 3 T is much lower than that on conventional SE sequence and (2) that 3DFSPGR is useless and cannot be applied to detect metastatic brain lesions because of the fatal low detectability in comparison with the conventional SE sequence. The purpose of the present study is to compare the enhancement effect of 3DFSPGR imaging with SE T1-WI of brain metastases using 3T MRI and to discover whether our hypotheses can be proven.

MATERIALS AND METHODS

Time-Dependent Changes in the Image Contrast of Brain Metastases

We initially undertook dynamic studies using 3DFSPGR imaging for 4 metastatic cases to investigate the

From the *Departments of Radiology, and †Radiologic Technology, School of Medicine, The University of Tokushima, Tokushima, Japan.

Received for publication December 21, 2006; accepted April 18, 2007.

Reprints: Kaori Furutani, MD, Department of Radiology, The University of Tokushima, 3-18-15 Kuramoto-cho, Tokushima 770-8503, Japan (e-mail: nm632934@blue.ocn.ne.jp).

Copyright © 2008 by Lippincott Williams & Wilkins

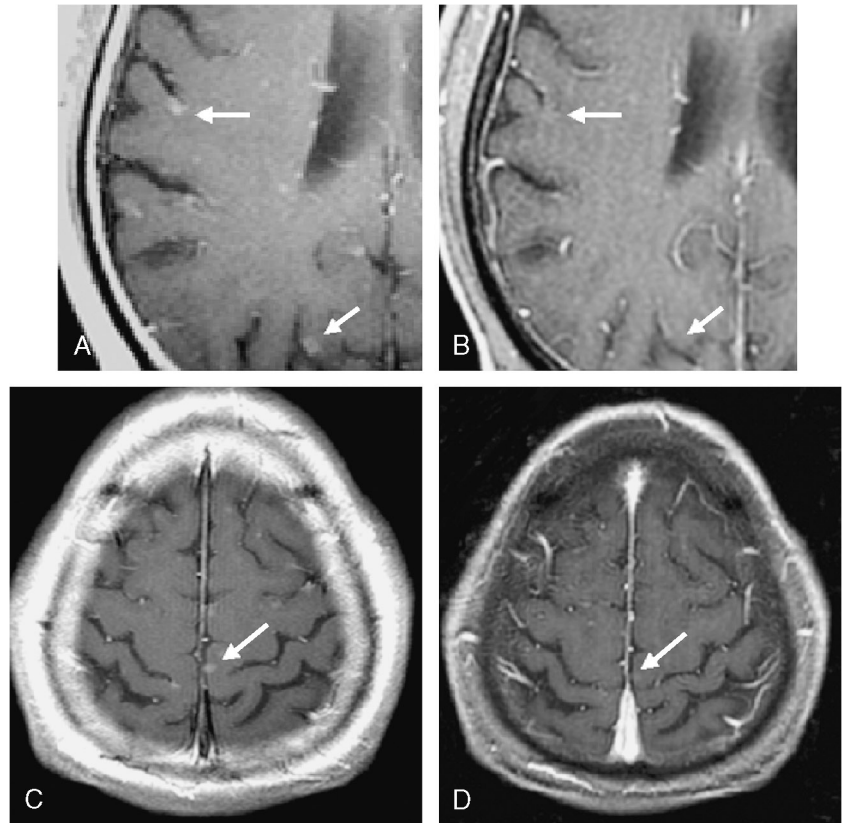


FIGURE 1. An example of reduced lesion conspicuity on FSPGR in a 59-year-old man with a brain metastasis from lung cancer. The FSPGR images were obtained before the SE images immediately after the administration of double-dose gadoteridol. Some of the lesions demonstrated on the SE images were either not seen or indistinct on the thin-slice FSPGR images (arrows).

time-dependent changes in the brain metastases after the administration of gadoteridol (Gd-HP-DO3A; Prohance, Eisai, Japan). The dose of gadoteridol administration was 0.2 mmol/kg (0.4 mL/kg), which is double the maximum dose permitted for clinical usage in Japan. After a bolus injection of gadoteridol at a rate of approximately 1.5 mL/s, we repeatedly obtained thin-slice SPGR images at 30-second intervals, including metastatic brain tumors on each scan image. The 4 subjects each underwent dynamic MRI studies, and one of the examples, shown in Figure 2A, was a 72-year-old man with a metastatic brain tumor secondary to renal cell carcinoma. We used a region of interest (ROI) to measure the signal intensity of the tumor on each image and calculated the increased ratio (the increased ratio = $[\text{post-SI} - \text{pre-SI}] / \text{pre-SI}$) and constructed a time-intensity curve (Fig. 2B).

The signal increase rate after gadoteridol injection was rapid and prominent at the initial phase until 60 seconds, and the changing rate of signal intensity 120 seconds after injection was much smaller than that in the initial phase, although some fluctuation were observed in the late phase depending on the cases. We considered that the changes in the enhanced effect of 120 seconds after injection was sufficiently small to be considered to have reached a plateau.

Patients

Sixty consecutive patients who underwent contrast-enhanced MRI for the detection of brain metastases between June and September 2005 were included in this study.

Eighty-one suspected metastatic brain tumors were present in 18 patients (8 men and 10 women; age range, 38–80, years; mean age, 62 years). Table 1 shows that 15 patients had lung cancer as the primary disease, whereas the other 3 patients had renal cell cancer, thyroid cancer, and breast cancer. None of the patients were treated with steroids, or none had poor cerebral circulation with any cerebral vascular abnormalities. All patients were injected with a double dose of gadoteridol (0.2 mmol/kg or 0.4 mL/kg). Our institutional review board approved the study, and informed consent was obtained from all patients.

Imaging Protocol

Magnetic resonance imaging was performed with a 3-T imager (Signa 3T Excite; GE Medical Systems) using a standard head coil. From the result of the advanced dynamic evaluation mentioned above, and under the consideration of clinical examination time, the interval after administration until postcontrast measurements was approximately 2 minutes from the end of the gadoteridol injection to minimize the time-dependent changes of the enhanced effect. The axial SE and 3DFSPGR T1-WIs were obtained in turn before and after administration of the gadoteridol injection, and the measurement order was not randomized in this study. Because our hypothesis was that the enhanced effect of GE imaging is much quite inferior to that of SE imaging, 3DFSPGR was given somewhat preferential treatment within the clinically permissible range, although the time-dependent

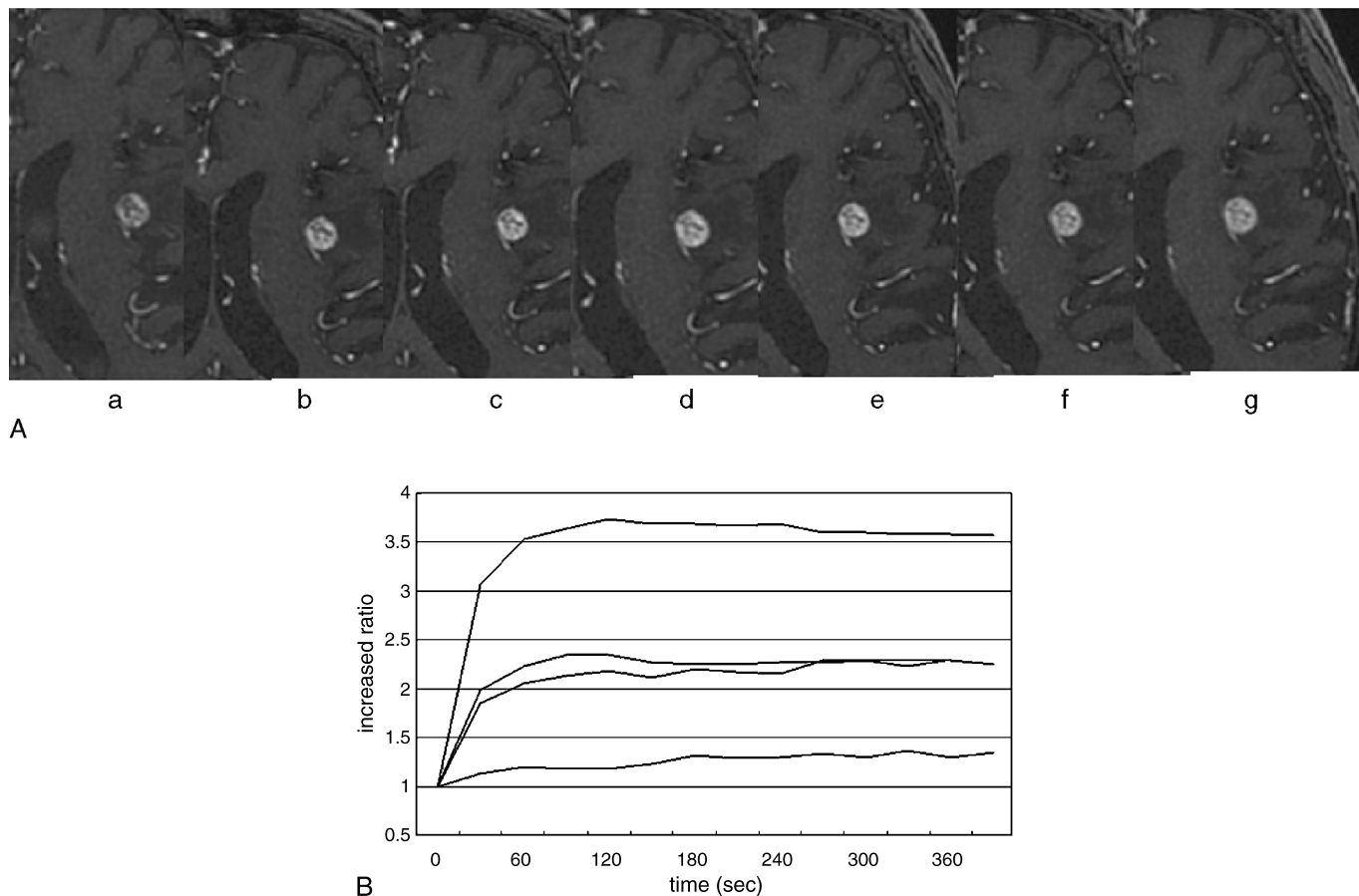


FIGURE 2. Dynamic study performed on a patient with 1 metastatic brain tumor from renal cell cancer. A, Thin slice FSPGR images that include the tumor were obtained at 30-second intervals; the displayed images were taken at the following times after the administration of double-dose gadoteridol (0.4 mL/kg): 30 (a), 60 (b), 90 (c), 120 (d), 150 (e), 300 (f), and 450 (g) seconds. The enhancement effect of the tumor increased gradually from a to d and then seemed to be stable from d to g. B, Time-intensity curve. The increased ratio of the tumor reached a peak at approximately 120 seconds (2 minutes) after the injection and remained high thereafter.

change of the enhanced effect was minimized by the measurement of the late phase. The standard parameters were set referring to the previous articles^{13,14} using 3 T as follows: for SE T1-WI, repetition time (TR)/echo time (TE), 625/14 milliseconds; slice thickness, 6.0 mm; field of view, 24 cm; matrix, 512 × 256; NEX, 1; scan time, 2.07 minutes, and for 3DFSPGR imaging, TR/TE, 9.8/4.2 milliseconds; slice thickness, 1.4 mm; field of view, 24 cm; matrix, 256 × 256; NEX, 1; flip angle, 18 degrees; scan time, 3.40 minutes. The 3DFSPGR images were reconstructed to provide thick slices (6 mm) of the same thickness as those of the SE T1-WI.

Statistical Analysis

We measured the signal intensity of the tumors on both the precontrast and postcontrast images for the SE, thick SPGR, and thin SPGR sequences using the ROI method (Fig. 3); the signal intensity of the normal brain close to the tumors on the postcontrast images was also measured. For the homogenous lesions, the ROI outlined the entire

lesion; for the inhomogeneous lesions, the area of maximal contrast enhancement was used. The enhancement rates and contrast rates were calculated according to the report by Rand et al⁶ following the below formulas:

$$\begin{aligned} \text{enhancement rate (\%)} &= (\text{postcontrast } SI_{\text{lesion}} - \text{precontrast } SI_{\text{lesion}}) \\ &\times 100 / \text{precontrast } SI_{\text{lesion}} \end{aligned}$$

$$\begin{aligned} \text{contrast rate (\%)} &= (\text{postcontrast } SI_{\text{lesion}} - \text{postcontrast } SI_{\text{brain}}) \\ &\times 100 / \text{postcontrast } SI_{\text{brain}} \end{aligned}$$

Statistical evaluation of the results was conducted using the paired *t* test.

RESULTS

The enhancement rate, contrast rate, and number of detected lesions are displayed in Table 2. For an equivalent thickness, both the enhancement and contrast rates on the thick FSPGR images were lower than those of the SE images

TABLE 1. Age, Sex, Primary Lesion, Dose, and Number of Tumors Detected for Patients in the Present Study

	Age	Sex	Primary Lesion	Gadoteridol	No. Tumors
1	75	Male	Lung cancer	Double dose	1
2	41	Male	Renal cell cancer	Double dose	9
3	77	Male	Lung cancer	Double dose	9
4	75	Female	Thyroid cancer	Double dose	3
5	55	Female	Lung cancer	Double dose	1
6	66	Male	Lung cancer	Double dose	2
7	67	Female	Lung cancer	Double dose	16
8	73	Female	Lung cancer	Double dose	2
9	57	Male	Lung cancer	Double dose	1
10	40	Female	Lung cancer	Double dose	6
11	67	Male	Lung cancer	Double dose	6
12	38	Female	Lung cancer	Double dose	1
13	71	Male	Lung cancer	Double dose	7
14	69	Male	Lung cancer	Double dose	11
15	58	Female	Breast cancer	Double dose	2
16	57	Female	Lung cancer	Double dose	2
17	49	Female	Lung cancer	Double dose	1
18	80	Female	Lung cancer	Double dose	1

($P < 0.05$) (thick FSPGR, $55 \pm 56\%$ and $30 \pm 35\%$; SE, $63 \pm 58\%$ and $36 \pm 38\%$, respectively). One lesion revealed on SE imaging was not observed on thick FSPGR imaging.

The enhancement rate, contrast rate, and detectability for thin-slice FSPGR imaging were all higher than those for SE imaging ($P < 0.01$) (thin FSPGR, $93 \pm 67\%$, $56 \pm 40\%$;

SE, $63 \pm 58\%$, $36 \pm 38\%$, respectively). This information is displayed in Figure 4.

DISCUSSION

We compared the enhancement effect of the FSPGR images with that of the SE images for detecting brain

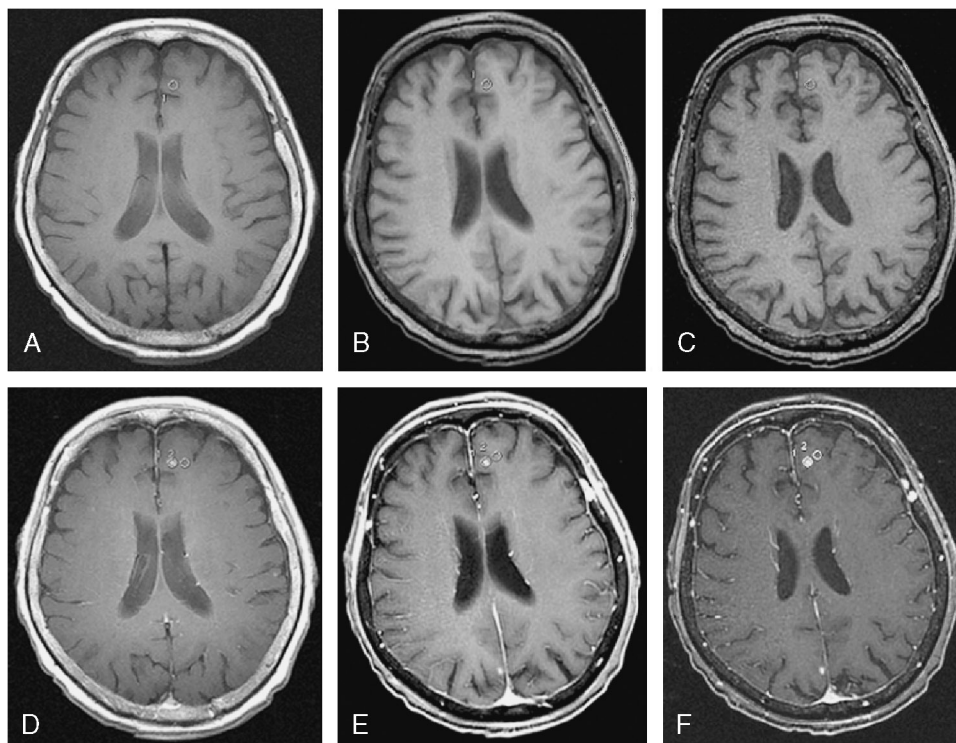


FIGURE 3. The ROI was placed over the same lesion in the precontrast and postcontrast images: (A and D) SE; (B and E) thick FSPGR; (C and F) thin FSPGR images and was also placed over the normal brain close to the tumor on the postcontrast images: (D) SE, (E) thick FSPGR, and (F) thin FSPGR images.

TABLE 2. Number of Detected Tumors and the Mean ± SD of the Measurements for the Signal Intensity, Enhancement, and Contrast Rates for SE, Thick FSPGR (6 mm), and Thin FSPGR (1.4 mm) T1-WIs

	Number	SI Precontrast (Lesion)	SI Postcontrast (Lesion)	SI Postcontrast (Brain)	Enhancement Rate, %	Contrast Rate, %
SE	79	828 ± 193	1307 ± 456	962 ± 156	63 ± 58	36 ± 38
FSPGR (6-mm thick)	78	1320 ± 201	1984 ± 543	1528 ± 113	55 ± 56*	30 ± 35*
FSPGR (1.4-mm thin)	81	1291 ± 187	2417 ± 665	1549 ± 124	93 ± 67**	56 ± 40**

Mean ± SD; **P* < 0.05; ***P* < 0.01.

metastases using 3T MRI. To the best of our knowledge, no studies have yet reported the differences in the enhancement effect between SE and 3DFSPGR imaging on 3T MRI.

In our study protocol, we started the postcontrast MRI measurement from 2 minutes after the Gd injection, according to the results of an advanced dynamic examination of the enhanced effect. Schorner et al¹⁵ showed the initial postcontrast measurement 8.5 minutes after the injection to reveal a maximum enhancement of the tumor, whereas Yuh et al¹⁶ reported that immediate (10 minutes) higher dose studies had the highest detection rate. These studies were conducted using conventional SE sequences, and they did not evaluate the fast changes soon after the injection. According to our results of the dynamic study using FSPGR, the changing rate in the early phase (until 90–120 seconds after the injection) was much more prominent, and the enhanced effect on most of the tumors nearly reached a plateau from 120 seconds after the injection. The interval between the end of the injection and the attainment of plateau in our study may seem short in comparison with the study by Yuh et al, but the difference in the subjects' physiques may be influential because the weight of our subjects was mainly ranged from 35 to 60 kg, which was considerably lower than that of Yuh et al.¹⁶

For the postcontrast measurements, 3DFSPGR imaging was conducted after SE imaging to provide somewhat preferential treatment within the clinically permissible range to confirm our hypothesis (ie, less enhanced effect of the GE sequence). However, we considered that the time-dependent effect would be minimized as a result of the advanced dynamic evaluation.

Despite the fact that 3DFSPGR imaging was conducted after SE imaging, the enhancement effect on the reconstructed FSPGR images with the same slice thickness as the SE images was lower than that on the SE images; our first hypothesis was confirmed. There have been some reports in which the enhanced effect on GE imaging was diminished in comparison with conventional SE T1-WI by clinical observation,^{3–5,8} and even theoretical analysis also showed that at a low Gd concentration, SE imaging showed greater enhancement than GE imaging.^{6,7} The reason for the low enhanced effect using gradient-echo T1-weighted sequences may not be simple, but Rand and Maravilla³ investigated this issue and concluded that the reduced contrast enhancement was related to the saturation effects (ie, the short repetition time of 3DFSPGR). Chappell et al⁵ reported that lesions are of relatively lower signal intensity than white matter on gradient-echo images

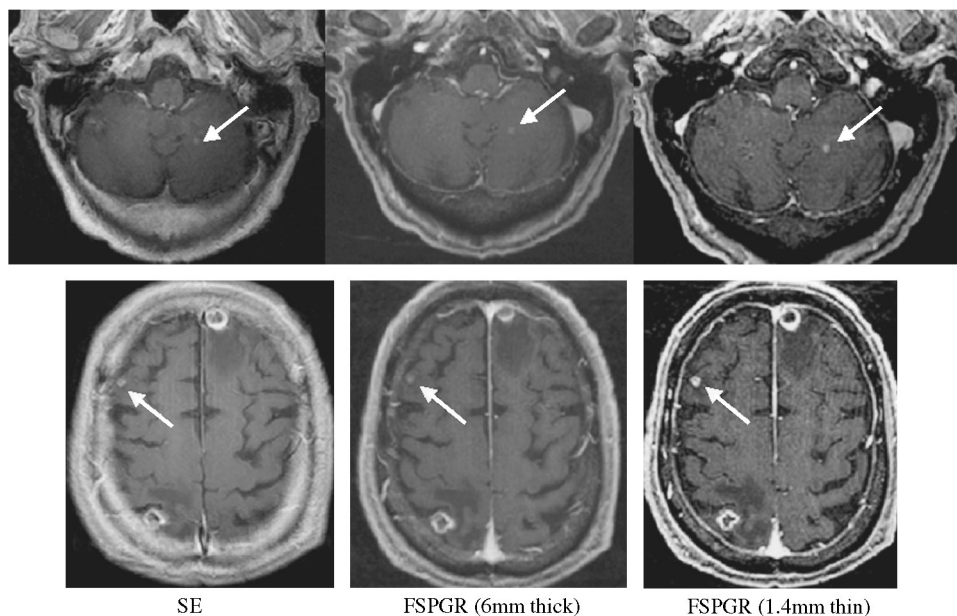


FIGURE 4. The lesions on the SE images are more conspicuous than those on the FSPGR images for the same thickness, but those on the thin-slice FSPGR images are more conspicuous, especially for the small lesions (arrows).

compared in comparison with SE T1-WIs; this lower baseline signal may make contrast enhancement more difficult to detect in white matter.

On the other hand, thin slice images by 3DFSPGR without reconstruction showed a greater increase in the enhancement effect and higher detectability than those by SE T1-WI in our study. Pui and Fok⁹ mentioned that the higher contrast-to-noise ratio of tumors on the contrast-enhanced SE images could not be found to be significant, and Mirowitz¹⁰ also described that there was not a significant difference in the quantitative contrast-to-noise measurement between 2-dimensional SE and 3D GE. Furthermore, Li et al¹¹ reported that small lesions were better visualized in the thin 3D GE images than in the thick SE images at 1.5 T. These results were closely consistent with those of our study at 3 T. Patrons et al¹² showed that SPGR had superior sensitivity to detect adrenocorticotropin-secreting pituitary tumors in comparison with SE despite the existence of the susceptibility phenomenon. Engh et al² suggested that 3DFSPGR with high-resolution and double-dose enhancement is a reliable method to evaluate the extent of intracranial disease in patients with known brain metastasis. The difference between thin slice and reconstructed images from 3DFSPGR occurred simply from the partial volume phenomenon by averaging signals in the pixels containing small lesions and normal tissues. The detectability of enhanced lesions between 3DFSPGR and SE depends on the size of the lesion. From the results of our study and consideration of the previous literature, our second hypothesis that 3DFSPGR is useless and cannot be applied to detect metastatic brain lesions could not be supported, and there were cases showing higher detectability by thin slice 3DFSPGR images than conventional SE images. It was considered that a decrease in the enhanced effect by GE imaging in comparison with SE imaging existed, but not to a fatal extent, and that the partial volume effect may sometimes be larger than the difference of the measurement sequences when the lesions are relatively small.

The influences of magnetic field strength and administration dose of contrast agents have been also evaluated by several previous studies.^{1,12,13,16,17} Nobauer-Huhmann et al¹³ showed a higher contrast between the tumor and the normal brain after the contrast agent's injection at 3 T than at 1.5 T; Ba-Ssalamah et al¹⁴ and Trattmig et al¹⁸ also described that the cumulative triple dose 3-T images showed the best results in comparison with the single-dose 3-T images and triple-dose 1.5-T images. In our study, we considered effective, even at 3 T, to apply a double dose of contrast agents to increase the enhanced effect and detectability. Unfortunately, a triple dose is not permitted for clinical usage by the Japanese government, and so it could not be examined.

Some reports have shown the use of magnetization transfer (MT) to have further increased the enhancement on some scans.^{8,19,20} Magnetization transfer imaging suppresses the normal tissue, and the conspicuousness of the gadolinium enhancement increases. Therefore, those areas of enhancement are better appreciated. However, at 3 T, the MT technique requires a high specific absorption rate and limits the slice numbers and the shortening of TR. Because of limited usage of the MT technique for routine clinical

examinations, we did not use MT in our study, and the issue of this technique remains for future work. Fishbach et al²¹ introduced inversion recovery techniques as well suited for T1-weighted imaging at 3 T, but it has been reported that inherent blurring can lead to a poor performance for very small brain lesions.

Our results and past reports indicate that the enhancement effect of gradient echo as 3DFSPGR images is consistently lower than that of SE images with the same slice thickness, despite the difference in magnetic field strength. We therefore should be aware of this characteristic even at 3 T and take care regarding the dose of contrast agents and scan timing after Gd injection when using SPGR sequences for T1-weighted imaging.

In conclusion, although the enhancement effect of the 3DFSPGR gradient echo is truly less than that of conventional SE T1-WIs, even on 3T MRI, this disadvantage effect by 3DFSPGR imaging will not be to a fatal degree at 3 T, and thin slice FSPGR images may play an important role in the detection of small metastatic lesions in routine clinical work with the appropriate high dose of contrast agent and the correct timing of the scans after injection.

REFERENCES

1. Trattmig S, Ba-Ssalamah A, Noebauer-Huhmann IM, et al. MR contrast agent at high-field MRI (3 Tesla). *Top Magn Reson Imaging*. 2003;14:365–375.
2. Engh JA, Flickinger JC, Niranjana A, et al. Optimizing intracranial metastasis detection for stereotactic radiosurgery. *Stereotact Funct Neurosurg*. 2007;86:162–168.
3. Rand S, Maravilla KR. Uses and limitations of spoiled gradient-refocused imaging in the evaluation of suspected intracranial tumors. *Top Magn Reson Imaging*. 1992;4:7–16.
4. Cheryman G, Golfieri R. Comparison of spin echo T1-weighted and FLASH 90 degrees gadolinium-enhanced magnetic resonance imaging in the detection of cerebral metastases. *Br J Radiol*. 1990;63:712–715.
5. Chappell PM, Pelc NJ, Foo TK, et al. Comparison of lesion enhancement on spin-echo and gradient-echo images. *AJNR Am J Neuroradiol*. 1994;15:37–44.
6. Rand S, Maravilla KR, Schmiedl U. Lesion enhancement in radio-frequency spoiled gradient-echo imaging: theory, experimental evaluation, and clinical implications. *AJNR Am J Neuroradiol*. 1994;15:27–35.
7. Mugler JP 3rd, Brookeman JR. Theoretical analysis of gadopentetate dimeglumine enhancement in T1-weighted imaging of the brain: comparison of two-dimensional spin-echo and three-dimensional gradient-echo sequences. *J Magn Reson Imaging*. 1993;3:761–769.
8. Elster AD. How much contrast is enough? Dependence of enhancement on field strength and MR pulse sequence. *Eur Radiol*. 1997;suppl 5: S276–S280.
9. Pui MH, Fok ECM. MR imaging of the brain: comparison of gradient-echo and spine-echo pulse sequences. *AJR Am J Roentgenol*. 1995;165:959–962.
10. Mirowitz SA. Intracranial lesion enhancement with gadolinium: T1-weighted spin-echo versus three-dimensional Fourier transform gradient-echo MR imaging. *Radiology*. 1992;185:529–534.
11. Li D, Haacke EM, Tarr RW, et al. Magnetic resonance imaging of the brain with gadopentetate dimeglumine-DTPA: comparison of T1-weighted spin-echo and 3D gradient-echo sequences. *J Magn Reson Imaging*. 1996;6:415–424.
12. Patrons N, Bulakbasi N, Stratakis CA, et al. Spoiled gradient recalled acquisition in the steady state technique is superior to conventional postcontrast spin echo technique for magnetic resonance imaging detection of adrenocorticotropin-secreting pituitary tumors. *J Clin Endocrinol Metab*. 2003;88:1565–1569.

13. Nobauer-Huhmann I-M, Ba-Ssalamah A, Mlynarik V, et al. Magnetic resonance imaging contrast enhancement of brain tumors at 3 Tesla versus 1.5 Tesla. *Invest Radiol.* 2002;3:114–119.
14. Ba-Ssalamah A, Nobauer-Huhmann IM, Pinker K, et al. Effect of contrast dose and field strength in the magnetic resonance detection of brain metastases. *Invest Radiol.* 2003;38:415–422.
15. Schorner W, Laniado M, Niendorf HP, et al. Time-dependent changes in image contrast in brain tumors after gadolinium-DTPA. *AJNR Am J Neuroradiol.* 1986;7:1013–1020.
16. Yuh WTC, Tali ET, Nguyen HD, et al. The effect of contrast dose, imaging time, and lesion size in the MR detection of intracerebral metastasis. *AJNR Am J Neuroradiol.* 1995;16:378–380.
17. Akeson P, Vikhoff B, Stahlberg F, et al. Brain lesion contrast in MR imaging. Dependence on field strength and concentration of gadodiamide injection in patients and phantoms. *Acta Radiol.* 1997;38:14–18.
18. Trattinig S, Pinker K, Ba-Ssalamah A, et al. The optimal use of contrast agents at high field MRI. *Eur Radiol.* 2006;16:1280–1287.
19. Wolff S, Balaban RS. Magnetization transfer imaging: Practical aspects and clinical applications. *Radiology.* 1994;192:593–599.
20. Duvvuri U, Roberts DA, Leigh JS, et al. Magnetization transfer imaging of the brain: a quantitative comparison of results obtained at 1.5T and 4.0T. *J Magn Reson Imaging.* 1999;10:527–532.
21. Fishbach F, Bruhn H, Pech M, et al. Efficacy of contrast medium use for neuroimaging at 3.0T. *J Comput Assist Tomogr.* 2005;29:499–505.